Exp Brain Res (2005) 164: 411–422
DOI 10.1007/s00221-005-2259-0

RESEARCH ARTICLE

**Arthur C. Leuthold · Frederick J. P. Langheim
Scott M. Lewis · Apostolos P. Georgopoulos**

Time series analysis of magnetoencephalographic data during copying

Received: 1 September 2004 / Accepted: 10 December 2004 / Published online: 28 April 2005

Abstract We used standard time series modeling to analyze magnetoencephalographic (MEG) data acquired during three tasks. Each task lasted 45 s, for a total data acquisition period of 135 s. Ten healthy human subjects fixated their eyes on a central blue point for 45 s (fixation only, "F" task). Then a pentagon (visual template) appeared surrounding the fixation point which simultaneously became red (fixation + template, "FT" task). After 45 s, the fixation point changed to green, which was the "go" signal for the subjects to begin continuously copying the pentagon for 45 s using a joystick and without visual feedback of their movement trajectory (fixation + template + copying, "FTC" task). MEG data were acquired continuously from 248 axial gradiometers at a sampling rate of 1017.25 Hz. After removal of cardiac artifacts and rejection of records with eyeblink artifacts, a Box–Jenkins autoregressive integrative moving average (ARIMA) analysis was applied to the unsmoothed, unaveraged MEG time series for model identification and estimation within 25 time lags (~25 ms). We found that an ARIMA model of 25th order autoregressive, first order differencing, and first order moving average ($p=25$, $d=1$, $q=1$) adequately modeled the series and yielded residuals practically stationary with respect to their mean, variance, and autocorrelation structure. These "prewhitened" residuals were then used for assessing pairwise associations between series using crosscorrelation analysis with ± 25 time lags ($\sim \pm 25$ ms). The cross-correlograms thus obtained revealed rich and consistent patterns of interactions between series with respect to positive and/or negative correlations. The overall prevalence of these patterns was very similar in the three tasks used, and, for particular sensor pairs, they tended to be preserved across tasks.

Keywords Magnetoencephalography · MEG · Time series · ARIMA · Copying

A. C. Leuthold · F. J. P. Langheim
S. M. Lewis · A. P. Georgopoulos (✉)
The Domenici Research Center for Mental Illness,
Brain Sciences Center, Veterans Affairs Medical Center,
One Veterans Drive, Minneapolis,
MN 55417, USA
E-mail: omega@umn.edu
Tel.: +1-612-725-2282
Fax: +1-612-725-2291

A. C. Leuthold · A. P. Georgopoulos
Department of Neuroscience,
University of Minnesota Medical School,
Minneapolis, MN 55455, USA

F. J. P. Langheim · A. P. Georgopoulos
MD/PhD Program,
University of Minnesota Medical School,
Minneapolis, MN 55455, USA

F. J. P. Langheim · A. P. Georgopoulos
Graduate Program in Neuroscience,
University of Minnesota, Minneapolis,
MN 55455, USA

S. M. Lewis · A. P. Georgopoulos
Department of Neurology,
University of Minnesota Medical School,
Minneapolis, MN 55455, USA

A. P. Georgopoulos
Department of Psychiatry, University of Minnesota Medical School, Minneapolis, MN 55455, USA

A. P. Georgopoulos
Center for Cognitive Sciences, University of Minnesota,
Minneapolis, MN 55455, USA

Introduction

Magnetoencephalography (MEG) is a research tool that allows high temporal resolution, noninvasive recordings from the human cortex. The MEG signal is the magnetic analog of the electroencephalographic (EEG) signal and derives from the same source, namely postsynaptic currents in pyramidal cells. The two methods share essentially unlimited temporal resolution. Recorded EEG potentials are spread widely and distorted by the conductivity patterns of the head. In contrast, magnetic

signals pass largely unaffected through bone and soft tissue, which allows MEG to localize sources with greater accuracy. In addition, the raw MEG signal recorded from a given sensor reflects a more predictable mixing of brain signals, a feature of special relevance to the present work. The primary disadvantage of MEG is decreased sensitivity with respect to deep sources and to a minority of sources with currents parallel to the surface of the head (Hillebrand and Barnes 2002). In general, source localization depends on different assumptions, according to the method used (for instance, the presence of single or multiple sources, the shape of the skull, and so on), and relies on rather subjective criteria (such as the level of goodness of fit for accepting a particular dipole). Localization is much more certain with functional imaging techniques, including functional magnetic resonance imaging (fMRI) and positron emission tomography (PET).

In addition to source localization, various frequency-domain analyses have been used to analyze the MEG signal (see Lounasmaa et al 1996; Pfurtscheller et al 2000). Neurons in the cortex have been found to show intrinsic oscillations, which are believed to sum to the persistent oscillations seen in EEG and MEG recordings (Llinas 1988; Steriade and Llinas 1988; Steriade et al 1990). Some timing information can be obtained from event-related desynchronization (ERD) and event-related synchronization (ERS) analyses. These terms refer to the decrease (ERD) or increase (ERS) of power in a specified frequency band in response to a stimulus or action (Pfurtscheller and Lopes da Silva 1999). For example, a decrease of the mu rhythm in the primary somatosensory cortex has been observed during median nerve stimulation (Nikouline et al 2000). Examples of increased synchronous activity have also been reported. Specifically, an increase of frontal theta rhythm has been observed during working memory and maze navigation tasks (Kahana et al 1999; Klimesch 1999; De Araujo et al 2002; Jensen and Tesche 2002), and an increase of gamma activity has been observed during cognitive tasks (Pfurtscheller and Lopes da Silva 1999; Rodriguez et al 1999). Gamma is the only common rhythm high enough in frequency to potentially reflect cortical binding (Miltner et al 1999; Pfurtscheller et al 2000; Varela et al 2001).

The study of interactions between distinct regions by spectral methods is limited to the presence of coherence and its phase relationship, with poor ability to determine direction of influence. Few studies have analyzed raw EEG data using time-domain methods, such as cross-correlation (Gevins et al 1981; Bressler 1995). In a recent MEG study (Gross et al 2001), cross-correlation analysis was performed on data derived using an adaptive beamformer spatial filter, instead of raw sensor data. Although such preprocessing of the data would reduce the mixing of sources and allow deeper sources to be isolated, issues concerning potential artificial correlations introduced by spatial filtering were not addressed in that study; moreover, the bandwidth used was less than 50 Hz and possible interactions at higher frequencies were not investigated. In addition, for the smaller, weaker sources producing the high frequencies used in this analysis, the signal-to-noise ratio (SNR) is too low to allow the isolation of sources by spatial filtering.

In the present study, we used time-domain, Box–Jenkins autoregressive integrative moving average (ARIMA) modeling (Box and Jenkins 1970) to analyze MEG data obtained during performances of three distinct visuomotor tasks, focused on short-term interactions, ranging from −25 to +25 ms. Specifically, we sought (a) to determine the structure of the time series by fitting appropriate autoregressive, differencing and moving average components, (b) to apply the model thus obtained to derive "prewhitened" residuals of the series (time series of residuals close to stationary, white noise), (c) to estimate pairwise interactions between series using the cross-correlation function (CCF), and (d) to compare quantitatively the prevalence of different CCF patterns across the three behavioral tasks used. Unlike methods based on frequency-domain analyses, such as coherence (which can take values from 0 to +1), cross-correlation can provide valuable information concerning the kind of influence (depending on the sign of the cross-correlation, ranging from −1 to +1).

Materials and methods

Subjects

Ten right-handed subjects (five women and five men) participated in these experiments as paid volunteers (age range 23–41 years; mean ± SD, 30 ± 6 years). Handedness was ascertained via the Edinburgh Handedness Inventory (Oldfield 1971). The study protocol was approved by the appropriate institutional review boards. Informed consent was obtained from all subjects according to the Declaration of Helsinki.

Experimental paradigm

Stimuli were generated by a computer and presented to the subjects using a LCD projector. Subjects performed three 45-s tasks in a consecutive order (Fig. 1) (Lewis et al 2003). In the first task (fixation only, "F"), they fixated a blue spot of light in the center of a black screen; in the second task (fixation + template [FT]), the light changed to red and a single white shape of a pentagon appeared around it; in the third task (fixation + template + copying [FTC]), the light changed to green (a "go" signal) and the subjects drew the shape continuously by moving an X–Y joystick with their right hand. Subjects were instructed to fixate during all tasks and to draw in the third task. They were also instructed to copy the shapes counterclockwise at their own speed; no visual feedback was provided. These three tasks were presented to the subjects in the same order, for we

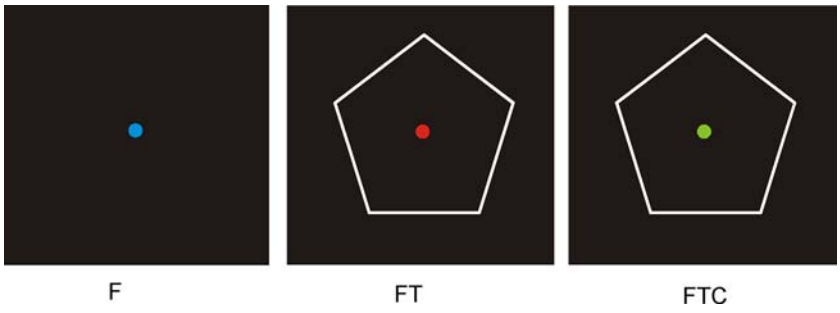

Fig. 1 The three tasks (see text for details)

wanted to explicitly investigate the presence of motor preparation effects during the FT period, and this could only be accomplished by having this and the copy task in sequence.

The fixation point and pentagon were presented to the subjects using a periscopic mirror system which placed the image on a screen approximately 62 cm in front of the subject's eyes. The pentagon subtended approximately 10° of the visual field.

Data acquisition

Magnetoencephalography

Data were collected using a 248-channel axial gradiometer MEG system (Magnes 3600WH, 4D-Neuroimaging, San Diego, CA, USA) (Fig. 2). The cryogenic helmet-shaped dewar of the MEG was located within an electromagnetically-shielded room to reduce noise. Data were acquired at 1017.25 Hz and filtered down to 0.1–400 Hz during acquisition. To insure against subject motion, five signal coils were digitized prior to MEG acquisition and consecutively activated before and after data acquisition, thereby locating the head in relation to the sensors. >

Hand movements

The *X*–*Y* output of the joystick was sampled at the same rate as the MEG data (at 1017.25 Hz) and was incorporated into the MEG data file, assuring correct time alignment.

Eye movements

Eye movements were recorded using the electrooculogram (EOG). Three electrodes were placed at locations around the right eye of each subject. The EOG signal was sampled at the same rate as above.

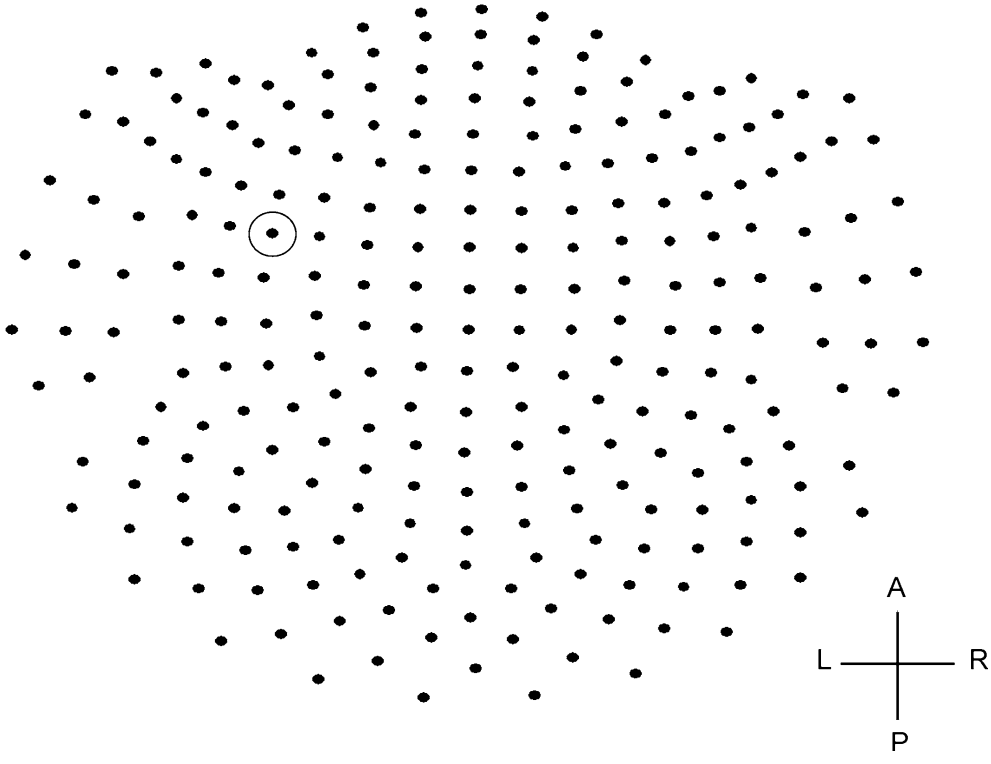

Fig. 2 Two-dimensional projection of the 248 sensor layout. *Encircled sensor* denotes the sensor (#67) for which data are illustrated in Figs. 3, 4, 5, 6, 7, 8, and 9. *L* left, *R* right, *A* anterior, and *P* posterior

Data analysis

The acquired MEG data were time series consisting of ~45,000 values per task, subject, and sensor. The cardiac artifact was removed from each series using event-synchronous subtraction (Leuthold 2003). Potential artifacts from eye-blinks and eye-movements were addressed by removing from analysis all data from sensors with $>100\ fT/\sqrt{\text{Hz}}$ power in the frequency band of 0–1 Hz.

Time series modeling

A major objective of these studies was to assess the interactions between time series in pairs of sensors. For that purpose, individual series need to be stationary, in other words "prewhitened" (Box and Jenkins 1970). Otherwise, nonstationarities in the series themselves can lead to erroneous associations (Box and Jenkins 1970; Priestley 1981). Therefore, the first step in our analyses was to model the time series and derive stationary (or quasi-stationary) residuals which could then be used to compute pairwise association measures, such as cross-correlations. All analyses described below were performed on single-trial, unsmoothed and unaveraged data. A Box–Jenkins ARIMA modeling analysis (Box and Jenkins 1970) was performed using SPSS 11 (SPSS Inc., Chicago, IL, USA) to identify the temporal structure of the data time series. We carried out these analyses on ~43,000 time points, after discarding the first and last 1,000 points, to avoid potential interference from processes at the time of starting the task, or processes anticipating its end. First of all, autocorrelation (ACF) and partial autocorrelation (PACF) functions were plotted for up to 25 lags, corresponding to ~25 ms. (Given our sampling rate of 1017.25 Hz, one lag corresponds to 0.983 ms). This number of lags was chosen because our interest in this study was focused on relatively short-range interactions. The ACF and PACF were calculated using the appropriate double-precision functions of the IMSL statistical and mathematical library, called from FORTRAN programs (Compaq Visual Fortran Professional Edition, version 6.6B).

Inspection of ACFs and PACFs for different channels and tasks (illustrated in "Results", below) suggested the need for differencing. This need was reinforced by the presence of local trends in plots of the raw data. Therefore, as the first step, a first-order differencing was applied to all data series. Next, inspection of ACFs and PACFs of the differenced series indicated the presence of autoregressive (AR), and possibly moving average (MA) components. We assessed this problem by performing extensive fitting, followed by diagnostic checking, using the SPSS statistical package (SPSS for Windows, version 10.1.0, SPSS Inc., 2000). The major requirement for successful modeling was that the derived residuals had to be as close to stationarity as possible, as assessed by plotting and evaluating their ACFs and PACFs. The stationarity of the ACF was quantified as follows (Priestley 1981). Each ACF consisted of 25 values—the correlation coefficients for every lag (1–25 ms). We obtained standard errors for these correlation coefficients and a probability value for their statistical significance. We then counted the number of significant correlations and noted the lags they belonged to. This count can be regarded as an estimate of the stationarity of the residuals. More exactly, one would expect 1/25 (4%) values to be significant by chance alone, and, therefore, an autocorrelogram with just one significant value would point to a fairly stationary process. However, as mentioned above, our purpose was not necessarily to make our series totally stationary but to remove nonstationarities which would influence further analyses and obscure the results and interpretations of the cross-correlation analysis. For that purpose, it is usually sufficient for a time series to be made "quasi-stationary" (Priestley 1981). In this analysis, we set the criterion at greater than two significant autocorrelations per autocorrelogram, corresponding to a significance level of $P = 2/25 = 0.08$.

A different question concerns the order of the AR and MA parameters in the model (the number of AR and MA coefficients). In general, one should strive to model a series adequately using the minimum number of parameters, and this would be a good approach for a single series. However, in this study we had to deal with a large number of time series (248 sensors per subject × 10 subjects × 3 tasks = 7,440 series), and tailoring the model to each individual series would have been not only impractical but it would probably have hindered comparisons across conditions. Extensive initial exploration showed that certain aspects of the model were common to all series, including first-order differencing, first-order MA, and a few (for example, up to five) AR orders. However, there was a marked variation across series with respect to including higher AR orders which were statistically significant in some but not in others. For purposes of uniform processing, and since incorporating higher AR orders would not have harmed the model, we opted for using the same orders for all series (S. Zeger, personal communication), namely 25 AR (equal to the lags used) and first-order MA. Formally, then, this model was of the form ($P = 25$, $d = 1$, $q = 1$), where (p, d, q) correspond to AR, differencing, and MA orders, respectively.

Cross-correlation analysis

The CCF between sensor time series was computed at double precision for lags of ±25 ms (a total of 51 lags, including zero lag).

Results

ARIMA modeling of MEG data

Altogether, 7,440 time series (45-s-long single trials) were available for analysis (3 tasks × 10 subjects × 248

sensors). Of those, 31 (0.42%) were rejected due to the presence of eyeblink artifacts. The results of the modeling analysis are illustrated for the same sensor (#67) and subject and the three tasks in Figs. 3–8. Figure 3 illustrates data from the F task. It depicts 3-s-long series of raw data, differenced values, and residuals after applying the ARIMA (25,1,1) model. It can be seen that the raw series was obviously nonstationary with respect to its mean and variance; this nonstationarity was essentially eliminated after differencing, and the noise was further reduced after the ARIMA modeling. Figure 4 shows autocorrelation (upper panel) and partial autocorrelation (lower panel) functions for the same data shown in Fig. 3. It can be seen that (a) the raw data were highly nonstationary with respect to their autocorrelation, (b) this nonstationarity was reduced but not eliminated following differencing, but (c) it disappeared completely following ARIMA modeling. Figures 5 and 6 illustrate the same points for data obtained during the FT task, and Figs. 7 and 8 for data obtained from the FTC task. It can be seen that data were effectively reduced to indistinguishable stationary series following the ARIMA modeling. This finding held when the whole 45-s-long series were analyzed.

As mentioned in the "Methods" section, the time series of the ARIMA (25,1,1) residuals was regarded nonstationary when there were two statistically significant autocorrelations in the autocorrelogram. For each subject and task, we calculated the percentage of sensors where the residuals exceeded the criterion above. The overall mean (±SEM), across the 30 subject-tasks was 5.73 ± 0.665%. This low value attests to the effectiveness of the ARIMA model employed.

Cross-correlation analysis

Figure 9 illustrates the importance of prewhitening the data in order for accurate estimates of the CCF to be obtained. In the upper left panel, the CCF between two time series with raw data is plotted. It can be seen that it is composed of large, very highly statistically significant correlation values which extend widely across the whole lag span of ±25 ms. In contrast, the CCF computed

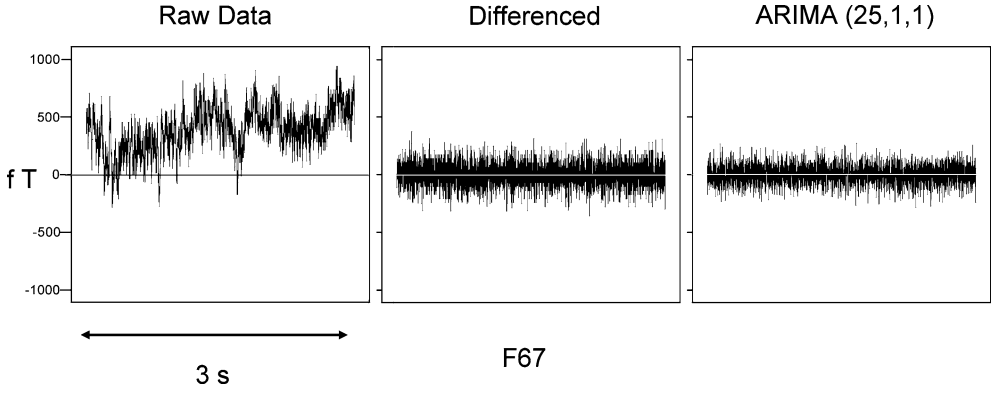

Fig. 3 F task. Data from sensor #67 (see Fig. 1) before and after the stated operations (see text for details). Data from a 3 s-segment (out of 45 s total) are illustrated. Notice the removal of trends present in raw data after differencing. Sampling interval is 0.98 ms

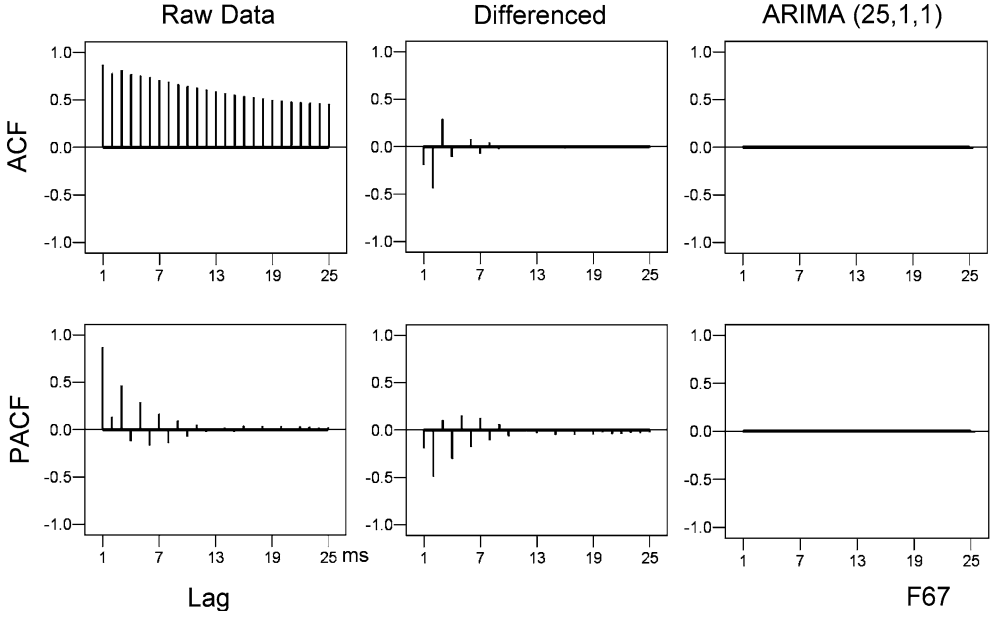

Fig. 4 F task. Autocorrelation (ACF) and partial autocorrelation (PACF) functions before and after the stated operations (see text for details). Notice the flat ACF and PACF after the ARIMA (25,1,1) modeling which indicates the effectiveness of the latter model. Sampling interval is 0.98 ms

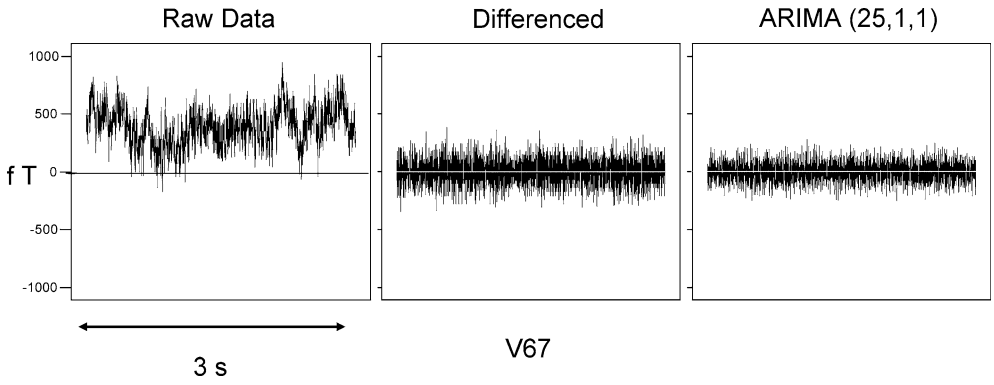

Fig. 5 FT task. Data from sensor #67 (see Fig. 1) before and after the stated operations (see text for details)

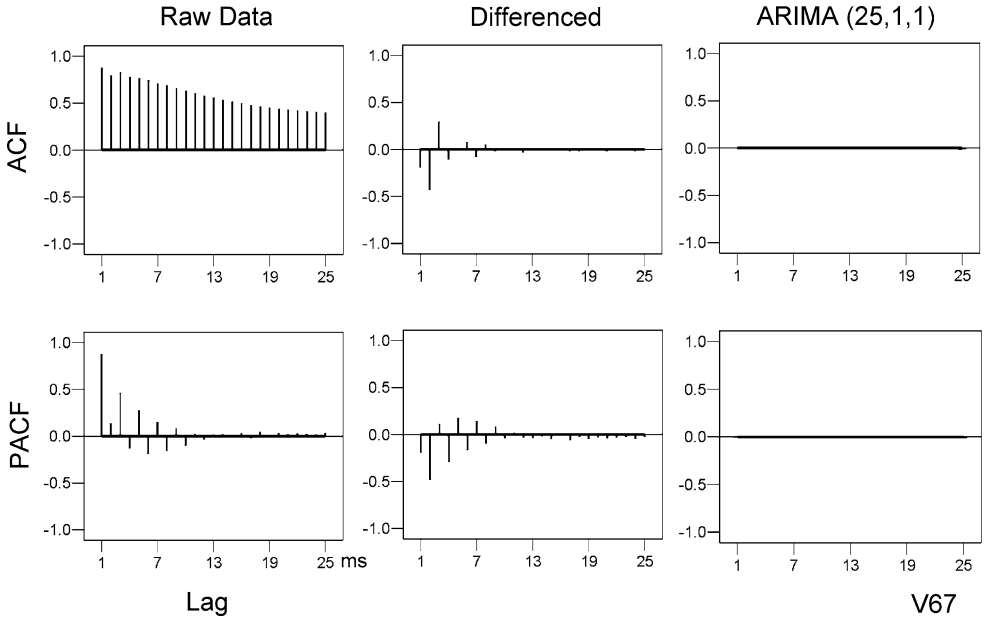

Fig. 6 FT task. ACF and PACF functions before and after the stated operations

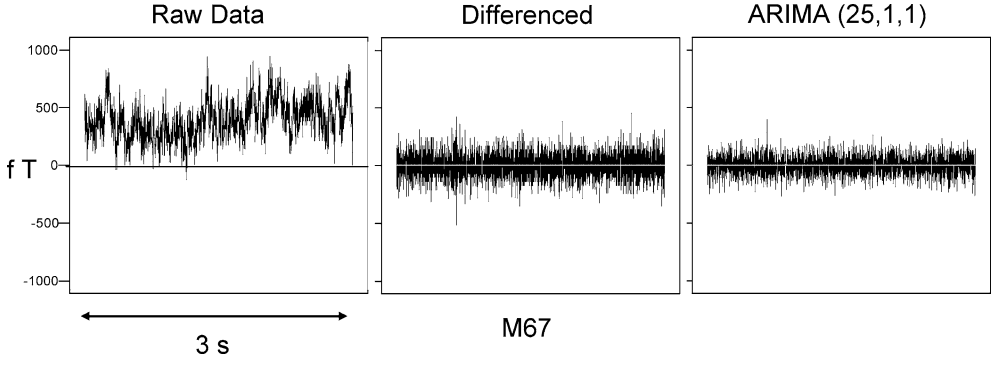

Fig. 7 FTC task. Data from sensor #67 (see Fig. 1) before and after the stated operations

using the "whitened" series of the residuals, after applying the ARIMA modeling, consists of much smaller correlation values extending to approximately ±4 ms around 0 (upper right plot); the same data are replotted on the right bottom panel at a higher resolution ordinate scale. It can be seen that, although smaller, these values clearly exceed the 95% confidence intervals of the correlation coefficients by a good margin. Obviously, the CCF computed from the raw data is erroneous, and reflects the typically highly autocorrelated structure of the individual series (see Figs. 4, 6, 8).

Figure 10 illustrates various patterns of CCF. Figures 11, 12, and 13 illustrate CCFs for different sensors in one subject during the FTC task. Based on the presence of a statistically significant peak and at least two temporally contiguous (in addition to the peak) and

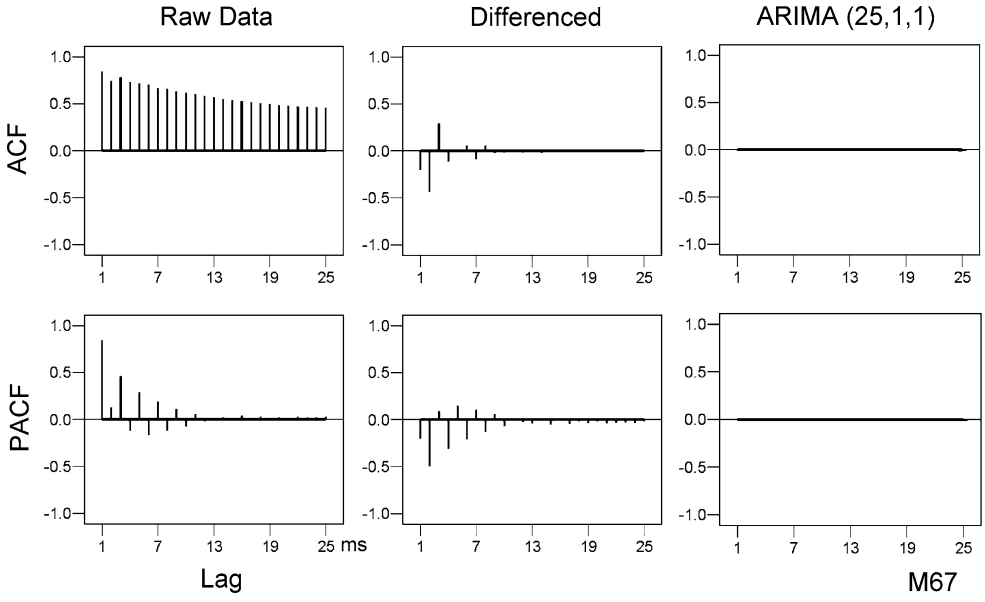

Fig. 8 FTC task. ACF and PACF functions before and after the stated operations

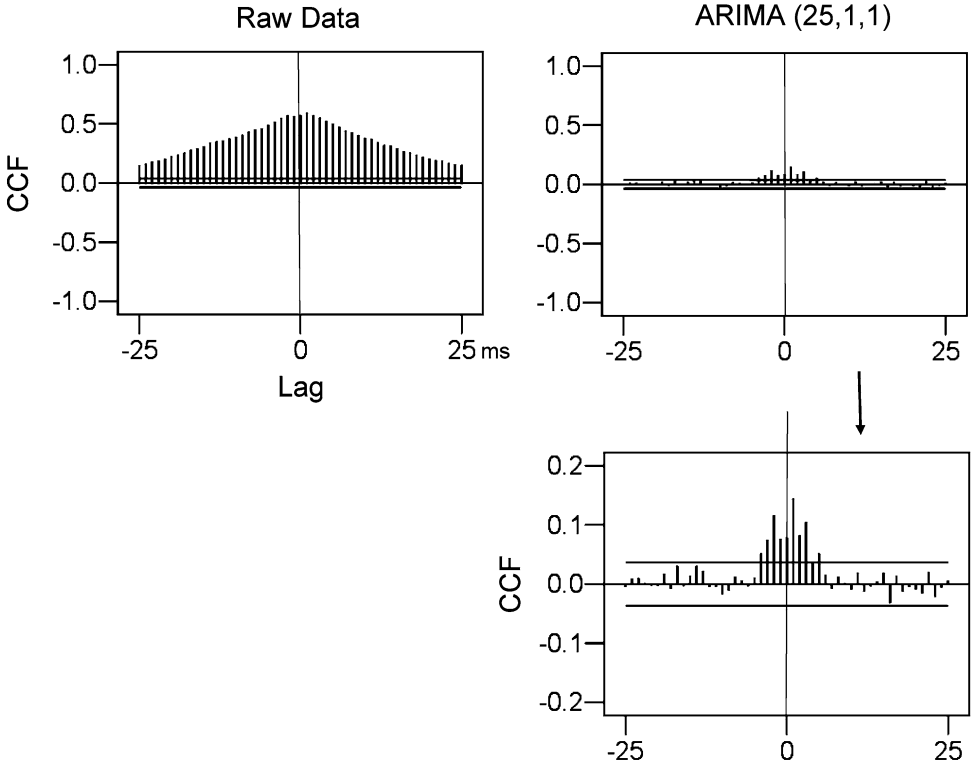

Fig. 9 Crosscorrelation functions (CCF) between two sensors in the FTC task before (raw data) and after the ARIMA (25,1,1) modeling. Notice the widespread positive CCF in Raw Data, reflecting obvious nonstationarities and significant ACF in the parent series (data not shown). The true CCF shows much more restricted statistically significant correlations (exceeding the 95% level of statistical significance). The plot in right bottom is the same as the one above it but at a finer scale

also statistically significant correlations of the same sign as the peak (positive or negative), we classified every cross-correlogram into one of four categories: (a) absence of effect, (b) presence of a positive correlation effect only, (c) presence of a negative correlation effect only, and (d) presence of both positive and negative correlation effects. Then we performed two kinds of analyses to determine possible task effects. First, we calculated the prevalence of these patterns in each task and compared the frequencies of occurrence of each pattern between tasks in two pairs of planned comparisons, namely the FT vs F, and FTC vs FT, using a chi-square analysis of the resulting 4×4 tables. We found that the tasks did not differ significantly in that respect. The overall prevalence of these patterns was as follows: (a) absence of effect, 27.2%; (b) presence of a positive correlation effect only, 27.9%; (c) presence of a negative correlation effect only, 38.3%; and (d) presence of both positive and negative correlation effects, 6.6%. In the second analysis, we computed the transition probabili-

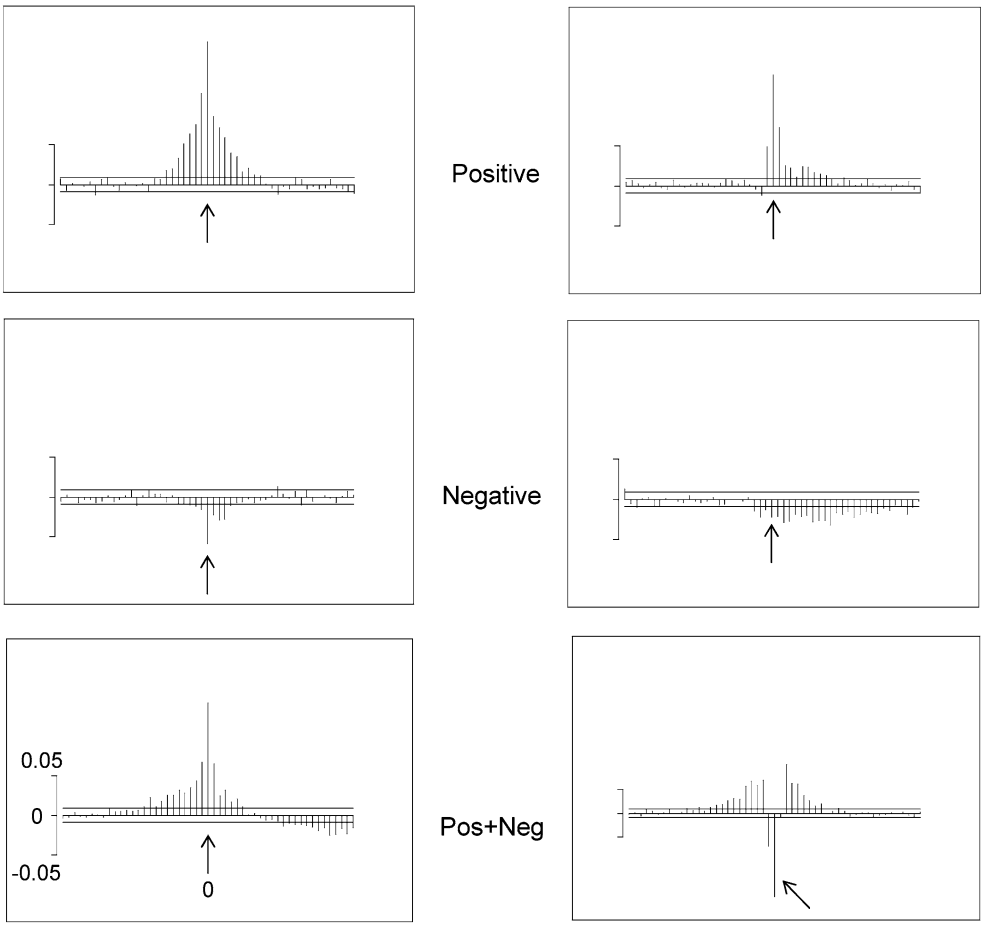

Fig. 10 Examples of some patterns of CCF observed for a lag of ±25 ms at intervals of 0.98 ms. *Vertical scale* CCF; *arrows* zero lag

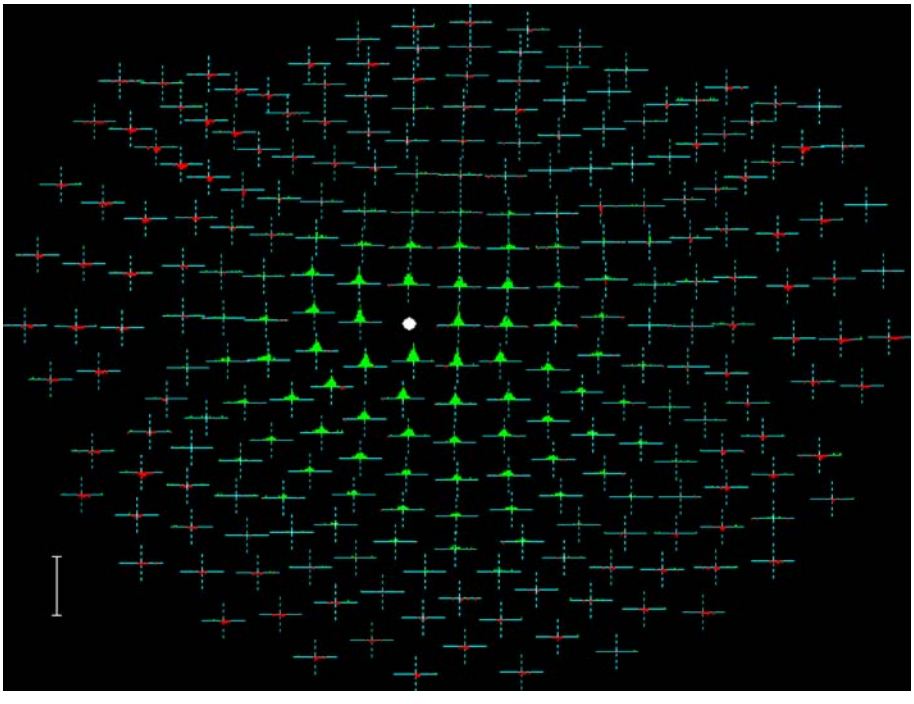

Fig. 11 CCFs (~±25 ms) between a centrally-located sensor (*white filled circle*) and all other sensors ($N = 247$). Data are from one subject performing the FTC task. *Green* and *red* denote positive and negative cross-correlations, respectively. *Dotted lines* indicate zero lag. *White vertical bars* indicate cross-correlation = 0.02

ties of each pattern to any other, for the transition from F to FT task, (Table 1) and from FT to FTC task (Table 2). We found that similar patterns tended to be conserved across tasks with respect to lack of effect and presence of positive or negative cross-correlations only. In contrast, the probability of transition from mixed

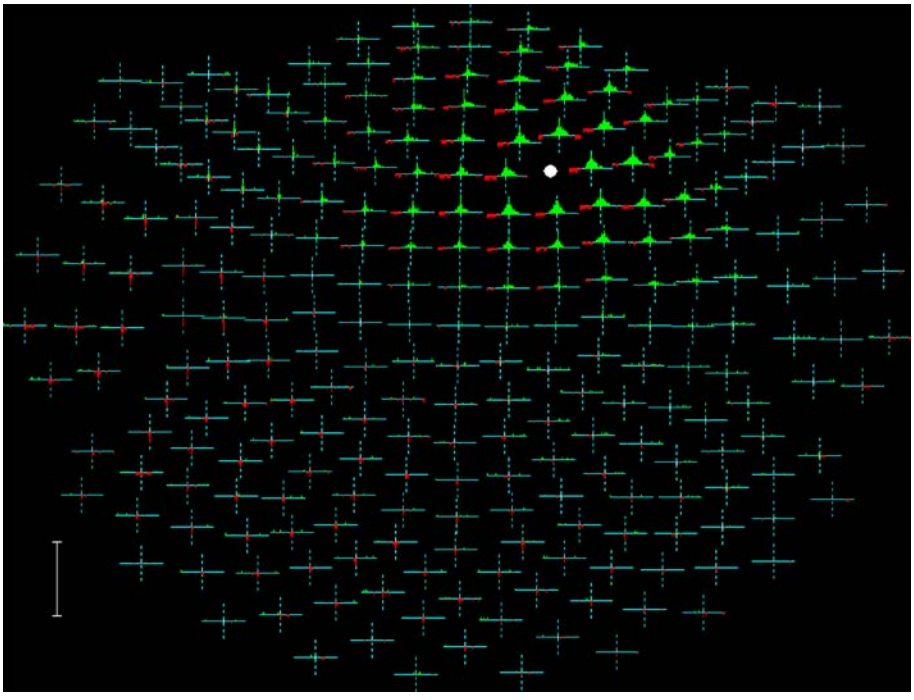

Fig. 12 CCFs between a right frontal sensor and all other sensors. Conventions are as in Fig. 11

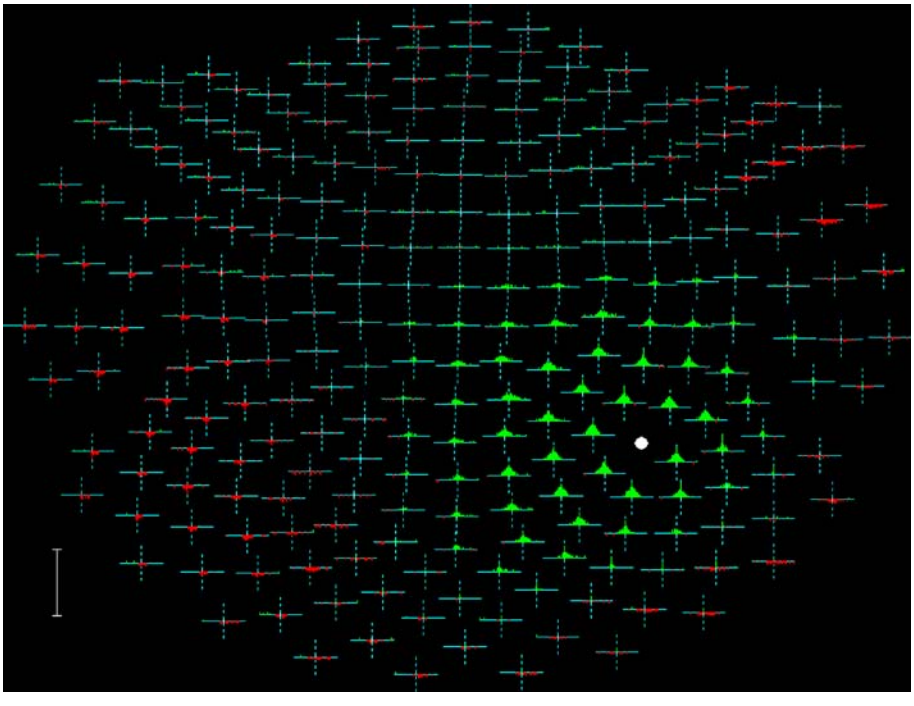

Fig. 13 CCFs between a right parietal sensor and all other sensors. Conventions are as in Fig. 11

Table 1 Transition probabilities (in %) for positive/negative cross-correlation patterns from F to FT task

		From: Fixation only			
		No effect	Positive only	Negative only	Positive + negative
To: Fixation + Template	No effect	70.3	7.8	13.6	4.2
	Positive only	7.1	82.2	0.8	28.9
	Negative only	21.7	1.4	80.1	29.1
	Positive + negative	0.9	8.5	5.5	37.8
	Total (%)	100	100	100	100

Table 2 Transition probabilities (in %) for positive/negative cross-correlation patterns from FT to FTC task

		From: Fixation only			
		No effect	Positive only	Negative only	Positive + negative
To: Fixation + Template	No effect	70.8	9.0	20.7	10.7
	Positive only	7.9	82.4	1.0	37.0
	Negative only	20.3	1.6	75.7	31.5
	Positive + negative	1.0	7.0	2.6	20.8
	Total (%)	100	100	100	100

(positive + negative) patterns to pure positive or negative effects was substantial, as well as the transition from no effect to a purely negative correlation.

Discussion

Methodological considerations

The MEG data analysis presented here relies on long time series and standard statistical methods, such as ARIMA modeling. We focused on time-domain analyses for two reasons. First, brain processes evolve in time, and we wanted to evaluate their relations in this domain. In contrast, frequency-domain analyses (such as spectral methods) destroy the temporal information, and, although time- and frequency-domain measures can ultimately be derived from one another (Jenkins and Watts 1968), results obtained by the two approaches retain the peculiarities of the approach and may prove to be more, or less, useful for a specific application. Second, we were specifically interested in assessing the dynamic interactions between signals recorded from different sensors, and for this purpose the CCF provides information on the sign of influence (the sign of the correlation -1 to $+1$); by contrast, the frequency-domain measure of association, namely the squared coherency (Jenkins and Watts 1968), can take only positive values.

We chose to investigate short-term interactions (within 25 ms) at high temporal resolution ($\sim$1 ms, sampling at 1017.25 Hz). It should be noted that this resolution is fully applicable to the assessment of the shift of a particular MEG series relative to another, and is independent of the frequency components present in the signal itself. For example, two signals consisting of only low frequencies can still be shifted, relative to one another, by a very small time; the shortest shift that can be estimated experimentally is equal to the sampling interval. Therefore, our high frequency sampling not only captured all of the information in the MEG signal (up to the upper limit of 400 Hz allowed by the settings of the collection protocol) but it also enabled the measurement of temporal shifts between series down to 1 ms.

ARIMA modeling

The first step in our analysis was to model the MEG time series using ARIMA (Box and Jenkins 1970). In order to perform an accurate statistical study of the relationships between time series data it is imperative to remove any autocorrelation structure from the original time series. Indeed, it can be easily demonstrated that uncorrelated data sets of the same autoregressive order will lead to spurious correlations when working with unfiltered data (Jenkins and Watts 1968). Identification of time series structure in the form of autocorrelation, partial autocorrelation and trends, may be achieved through the use of Box–Jenkins ARIMA modeling (Box and Jenkins 1970). This linear modeling procedure combines autoregression, differencing and moving averages to represent a time series. It was described by Box and Jenkins as an iterative method composed of observation of autocorrelation functions, estimation of parameters, and diagnostic review. Given the nature of the MEG signals recorded for this study, first-order differencing of the data was necessary. After extensive ARIMA modeling, we determined that an ARIMA (25,1,1) model was universally effective at accounting for the temporal structure of practically all of our series. This model included 25 orders autoregressive, a first-order differencing, and a first-order moving average component. The autoregressive and differencing components are linear; the former denotes a dependence of a given value on its preceding values, whereas the latter denotes the presence of linear trends. The presence of such effects is not surprising since significant autoregressive components are common in any time series, and linear trends commonly denote the effect of a factor influencing the series. On the other hand, the presence of a low (first)-order moving average component, a nonlinear effect, is also common in time series and denotes a minimal influence on a given value w_t of fluctuations in the immediately preceding values $w_{t\text{-}1}$. Overall, then, these results indicate that the processes generating the MEG series are, at least in the context of these experiments, essentially linear and very similar across the three tasks used.

With the advent of whole-head MEG, a noninvasive technique for the study of high frequency interactions in the human brain became available. However, to our knowledge, little work has been carried out exploring the temporal dynamics of raw MEG signals from single sensors. Indeed, the majority of MEG and EEG research directed toward temporal dynamics has focused on short window interactions, and/or narrow frequency bands using cross-spectral and/or cross-correlation studies (Andrew and Pfurtscheller 1996; Herculano-Houzel et al

1999; Mitra and Pesaran 1999; Ding et al 2000; Gross et al 2001; Fries et al 2002; Yamagishi et al 2003, for examples). It should be noted that the condition of stationarity or quasi-stationarity is a requirement for association analyses in both the time- and frequency-domains. The overwhelming majority of the studies referred to above do not address the requirement of stationarity within a time series before embarking on comparisons between them, whereas those that address it often only do so by using short temporal windows (Andrew and Pfurtscheller 1996; Tass et al 1998; Mitra and Pesaran 1999). However, in the latter case, no statements can be made on the association between two time series with respect to longer time periods.

Temporal interactions: cross-correlation and sampling frequency

The successful ARIMA modeling of the MEG time series allowed the rigorous estimation of CCF and, therefore, the evaluation of pairwise interactions between various sensors. Within the range of time lags we investigated ($\sim\pm 25$ ms), the prevalence of overall CCF patterns was clear-cut and stable across the three behavioral tasks. Specifically, the least frequent pattern was a combination of positive and negative interactions (7%), absence of significant interactions was more prevalent (27%), whereas the presence of only one kind of interaction (positive or negative) was most frequent (28 and 38%, respectively). It is also noteworthy that these patterns from one task to another tended to be conserved, although absence of significant interaction tended to become purely negative, while combined positive and negative interactions tended to become either purely positive or purely negative, from F to FT to FTC.

A different issue concerns the temporal resolution of interactions. It can be seen in Fig. 10 that the magnitude and sign of interactions observed can vary appreciably from millisecond to millisecond, as was commonly the case in many other instances. This finding justifies the high-frequency sampling of the MEG signal and draws attention to the importance of the sampling frequency for considerations other than recovery of the signal itself. This latter objective has traditionally been the main motivation in MEG work. For example, the common practice of filtering down the MEG signal to, say, 45 Hz (see Streit et al 1999), relies on the observation that most of the power in typical MEG time series is found up to $\sim$50 Hz. However, it does not follow from this that higher frequencies are useless. First of all, the argument that "information lies where the power is" is misleading. Consider music, as an example: most of the power is found in the low frequencies, and, in fact, the more low or very low frequencies a piece contains, the higher the percentage of the total power allocated to these frequencies; and yet, the melody is typically present in the mid-range. If we were to apply the principle of "filter down to where most of the power is" to music, practically all interesting music would be effectively eliminated. Although high sampling rates have been used in some recent studies (see, for example, Alary et al 2002; Ioannides et al 2004), this is not common practice. In addition, there are a few reports in the literature on very high frequency responses (600 Hz) induced by somatosensory stimulation, but none was concerned with correlation or coherence (Curio et al 1997; Gobbele et al 1999; Sakuma et al 1999).

Here we documented a different good reason for using a very high sampling frequency (1017.25 Hz), namely as means to assess the interactions between MEG signals at the millisecond resolution. Commonly, the high temporal resolution of the MEG is touted as one of its major advantages, and yet only lip service is paid to this advantage, since filtering the MEG signal down to, say, 40 Hz essentially reduces this resolution to 25 ms. The sampling frequency needed to detect an arbitrarily short time shift between two time series depends on the value of the time shift desired to be detected and not on the frequency content of the signal itself. The fact that 1-ms shifts can result in major changes in correlation (Fig. 10) documents the importance of high-frequency sampling and justifies its use.

Whereas it is true that relatively little MEG signal power exists above about 50 Hz, and information at the higher frequencies does not seem to contribute to conventional localization of sources, information about neural activity is still present at these higher frequencies. A method sensitive enough may be able to make use of this information. It should also be noted that, while the MEG signal power is very low above about 50 Hz, this is not necessarily a reflection of actual brain activity. Synchronous activity of 10,000 or more neurons is necessary for source localization (Hämäläinen et al 1993), but the large majority of the recorded signal is not from these few localizable sources. It is reasonable to expect that a larger population of neurons cannot fire coherently with the same precision as a smaller population of neurons. Since the sources are not in general synchronous, they do not tend to sum to produce large signals, as is seen at lower frequencies. The expectation then is that the smaller populations produce higher frequencies in the data.

The higher frequency information is likely a collection of a large number of small, weak sources. The SNR is greatest in the raw data, and a focusing method, such as the beamformer spatial filter, would substantially reduce the ability to see these weaker, high frequency sources. As mentioned above, due to the conductivity patterns of the head, the magnetic field from a source is much more confined than its electric signal. The detection coils used for the test data in this paper were first-order axial gradiometer coils (Williamson and Kaufman 1981), which further reduce sensitivity to distant sources. Given these considerations, MEG is the best tool for this work, and raw sensor data is most likely to provide the necessary SNR to see the higher frequency sources with minimal spreading of the signal.

Acknowledgements This work was supported by the MIND Institute (Albuquerque, NM), the Department of Veterans Affairs, and the American Legion Brain Sciences Chair.

References

Alary F, Simoes C, Jousmaki V, Forss N, Hari R (2002) Cortical activation associated with passive movements of the human index finger: an MEG study. Neuroimage 15:691–696

Andrew C, Pfurtscheller G (1996) Event-related coherence as a tool for studying dynamic interaction of brain regions. Electroencephalogr Clin Neurophysiol 98:144–148

Box GEP, Jenkins GW (1970) Time series analysis: forecasting and control. Holden Day, San Francisco, CA

Bressler SL (1995) Large-scale cortical networks and cognition. Brain Res Rev 20:288–304

Curio G, Mackert BM, Burghoff M, Neumann J, Nolte G, Scherg M, Marx P (1997) Somatotopic source arrangement of 600 Hz oscillatory magnetic fields at the human primary somatosensory hand cortex. Neurosci Lett 234:131–134

De Araujo DB, Baffa O, Wakai RT (2002) Theta oscillations and human navigation: a magnetoencephalography study. J Cogn Neurosci 14:70–78

Ding M, Bressler SL, Yang W, Liang H (2000) Short-window spectral analysis of cortical event-related potentials by adaptive multivariate autoregressive modeling: data preprocessing, model validation, and variability assessment. Biol Cybern 83:35–45

Fries P, Schroeder J-H, Roefsema PR, Singer W, Engel AK (2002) Oscillatory neuronal synchronization in primary visual cortex as a correlate of stimulus selection. J Neurosci 22:3739–3754

Gevins AS, Schaffer RE, Doyle JC, Cutillo BA, Tannehill RS, Bressler SL (1981) Shadows of thought: shifting lateralization of human brain electrical patterns during brief visuomotor task. Science 213:918–922

Gobbele R, Buchner H, Scherg M, Curio G (1999) Stability of high-frequency (600 Hz) components in human somatosensory evoked potentials under variation of stimulus rate–evidence for a thalamic origin. Clin Neurophysiol 110:1659–1663

Gross J, Kujala J, Hamalainen M, Timmermann L, Schnitzler A, Salmelin R (2001) Dynamic imaging of coherent sources: studying neural interactions in the human brain. Proc Natl Acad Sci USA 98:694–699

Hämäläinen M, Hari R, Ilmoniemi R, Knuutila J, Lounasmaa O (1993) Magnetoencephalography—theory, instrumentation and applications to noninvasive studies of the working human brain. Rev Mod Phys 65:413–497

Herculano-Houzel S, Munk MHJ, Neuenschwander S, Singer W (1999) Precisely synchronized oscillatory firing patterns require electroencephalographic activation. J Neurosci 19:3992–4010

Hillebrand A, Barnes GR (2002) A quantitive assessment of the sensitivity of whole-head MEG to activity in the adult human cortex. Neuroimage 16:638–650

Ioannides AA, Corsi-Cabrera M, Fenwick PB, del Rio Portilla Y, Laskaris NA, Khurshudyan A, Theofilou D, Shibata T, Uchida S, Nakabayashi T, Kostopoulos GK (2004) MEG tomography of human cortex and brainstem activity in waking and REM sleep saccades. Cereb Cortex 14:56–72

Jenkins GM, Watts DG (1968) Spectral analysis and its applications. Holden-Day, Oakland, CA

Jensen O, Tesche CD (2002) Frontal theta activity in humans increases with memory load in a working memory task. Eur J Neurosci 15:1395–1399

Kahana MJ, Sekuler R, Caplan JB, Kirschen M, Madsen JR (1999) Human theta oscillations exhibit task dependence during virtual maze navigation. Nature 3999:781–784

Klimesch W (1999) EEG alpha and theta oscillations reflect cognitive and memory performance: a review and analysis. Brain Res Rev 29:169–195

Leuthold AC (2003) Subtraction of heart artifact from MEG data: the matched filter revisited. Soc Neurosci Abstr 863.15

Lewis SM, Jerde TA, Tzagarakis C, Georgopoulos MA, Tsekos N, Amirikian B, Kim SG, Ugurbil K, Georgopoulos AP (2003) Cerebellar activation during copying geometrical shapes. J Neurophysiol 90:3874–3887

Llinas RR (1988) The intrinsic electrophysiological properties of mammalian neurons: insights into central nervous system function. Science 242:1654–1664

Lounasmaa OV, Hamalainen M, Hari R, Salmelin R (1996) Information processing in the human brain: magnetoencephalographic approach. Proc Natl Acad Sci USA 20:8809–8815

Miltner WH, Braun C, Arnold M, Witte H, Taub E (1999) Coherence of gamma-band EEG activity as a basis for associative learning. Nature 397:434–436

Mitra PP, Pesaran B (1999) Analysis of dynamic brain imaging data. Biophys J 76:691–708

Nikouline VV, Linkenkaer-Hansen K, Wikstrom H, Kesaniemi A, Antonova EV, Ilmoniemi RJ, Huttunen J (2000) Dynamics of mu-rhythm suppression caused by median nerve stimulation: a magnetoencephalographic study in human subjects. Neurosci Lett 294:163–166

Oldfield RC (1971) The assessment and analysis of handedness: the Edinburgh inventory. Neuropsychologia 9:97–113

Pfurtscheller G, Lopes da Silva FH (1999) Event-related EEG/MEG synchronization and desynchronization: basic principles. Clin Neurophysiol 110:1842–1857

Pfurtscheller G, Neuper C, Pichler-Zalaudek K, Edlinger G, Lopes da Silva FH (2000) Do brain oscillations of different frequencies indicate interaction between cortical areas in humans? Neurosci Lett 286:66–68

Priestley MB (1981) Spectral analysis and time series. Academic, San Diego, CA

Rodriguez E, George N, Lachaux JP, Martinerie J, Renault B, Varela FJ (1999) Perception's shadow: long-distance synchronization of human brain activity. Nature 397:430–433

Sakuma K, Sekihara K, Hashimoto I (1999) Neural source estimation from a time-frequency component of somatic evoked high-frequency magnetic oscillations to posterior tibial nerve stimulation. Clin Neurophysiol 110:1585–1588

Steriade M, Llinas RR (1988) The functional states of the thalamus and the associated neuronal interplay. Physiol Rev 68:649–742

Steriade M, Gloor P, Llinas RR, Lopes da Silva FH, Mesulam MM (1990) Report of IFCN committee on basic mechanisms. Basic mechanisms of cerebral rhythmic activities. Electroencephalogr Clin Neurophysiol 76:481–508

Streit M, Ioannides AA, Liu L, Wolwer W, Dammers J, Gross J, Gaebel W, Muller-Gartner HW (1999) Neurophysiological correlates of the recognition of facial expressions of emotion as revealed by magnetoencephalography. Cogn Brain Res 7:481–491

Tass P, Rosenblum MG, Weule J, Kurths J, Pikovsky A, Volkmann J, Schnitzler A, Freund HJ (1998) Detection of n:m phase locking from noisy data: application to magnetoencephalography. Phys Rev Lett 81:3291–3294

Varela F, Lachaux JP, Rodriguez E, Martinerie J (2001) The brainweb: phase synchronization and large-scale integration. Nat Rev Neurosci 2:229–239

Williamson SJ, Kaufman L (1981) Biomagnetism. J Magn Magn Mater 22:129–202

Yamagishi N, Callan DE, Goda N, Anderson SJ, Yoshida Y, Kawato M (2003) Attentional modulation of oscillatory activity in human visual cortex. Neuroimage 20:98–113